www.nature.com/aps

Acta Pharmacologica Sinica

ARTICLE

Garcinol inhibits esophageal cancer metastasis by suppressing the p300 and TGF-β1 signaling pathways

Jing Wang[1,2], Man Wu[2], Dan Zheng[2], Hong Zhang[2], Yue Lv[2], Li Zhang[2], Hong-sheng Tan[2], Hua Zhou[1], Yuan-zhi Lao[2] and Hong-xi Xu[1,2]

Metastasis causes the main lethality in esophageal cancer patient. Garcinol, a natural compound extracted from *Gambogic genera*, is a histone acetyltransferase (HAT) inhibitor that has shown anticancer activities such as cell cycle arrest and apoptosis induction. In this study, we investigated the effects of garcinol on the metastasis of esophageal cancer in vitro and in vivo. We found that garcinol (5–15 μM) dose-dependently inhibited the migration and invasion of human esophageal cancer cell lines KYSE150 and KYSE450 in wound healing, transwell migration, and Matrigel invasion assays. Furthermore, garcinol treatment dose-dependently decreased the protein levels of p300/CBP (transcriptional cofactors and HATs) and p-Smad2/3 expression in the nucleus, thus impeding tumor cell proliferation and metastasis. Knockdown of p300 could inhibit cell metastasis, but CBP knockdown did not affect the cell mobility. It has been reported that TGF-β1 stimulated the phosphorylation of Smad2/3, which directly interact with p300/CBP in the nucleus, and upregulating HAT activity of p300. We showed that garcinol treatment dose-dependently suppressed TGF-β1-activated Smad and non-Smad pathway, inhibiting esophageal cancer cell metastasis. In a tail vein injection pulmonary metastasis mouse model, intraperitoneal administration of garcinol (20 mg/kg) or 5-FU (20 mg/kg) significantly decreased the number of lung tumor nodules and the expression levels of Ki-67, p300, and p-Smad2/3 in lung tissues. In conclusion, our study demonstrates that garcinol inhibits esophageal cancer metastasis in vitro and in vivo, which might be related to the suppression of p300 and TGF-β1 signaling pathways, suggesting the therapeutic potential of Garcinol for metastatic tumors.

Keywords: garcinol; esophageal cancer; metastasis; histone acetyltransferase; TGF-β1; p300/CBP; Smad2/3

Acta Pharmacologica Sinica (2020) 41:82–92; https://doi.org/10.1038/s41401-019-0271-3

INTRODUCTION

Esophageal cancer is the eighth most common cancer in the world, and it has a poor prognosis and uneven geographic distribution [1]. There are two dominant histological types of esophageal cancer: esophageal adenocarcinoma and esophageal squamous cell carcinoma (ESCC). Historically, ESCC has shown a trend of increasing incidence in eastern Asia and Africa [2]. According to statistics from China, the United States and Europe, the 5-year survival rate of esophageal cancer is generally less than 21% [3–5]. Furthermore, over 50% of patients present with either unresectable tumors or radiographically visible metastases upon the preliminary diagnosis of esophageal cancer [6]. Cancer metastasis is the main cause of death among cancer patients [7]. Although chemoradiotherapy is the standard therapy for esophageal cancer and offers a statistically significant extension of survival, the therapeutic benefit of this treatment is unsatisfactory for most patients, and its potential for toxic effects should draw attention [8–10]. Thus, it is crucial to find an improved treatment strategy that impedes the development of this fatal disease.

Histone acetylation is an important protein modification. Usually, histone modification acts on the N-terminus of histones, altering gene transcription, translation and cell regulation [11, 12]. Histone acetyltransferases (HATs) and histone deacetylases (HDACs) antagonize each other to maintain a dynamic balance of histone acetylation levels and participate in gene expression regulation [13]. p300/CBP is an important member of a group of acetyltransferases that are ubiquitously expressed transcriptional coactivators. The abnormal expression of p300/CBP leads to a series of effects, such as the induction of tumor cell proliferation and metastasis [14, 15], and affects the activities of downstream pathways [15, 16]. While p300 is a closely related paralog of CBP, the functions of p300 and CBP are different [17]. The high expression of p300 is associated with poor prognosis and an unfavorable impact on survival in non-small cell lung cancer (NSCLC) [18] and ESCC patients [19]. Linc00460, which is upregulated by CBP/p300 through histone acetylation, promotes carcinogenesis in ESCC [20]. p300 and CBP may be new targets for the treatment of cancer and metastasis [21, 22].

Transforming growth factor-β (TGF-β) signaling enhances metastasis to promote malignancy during cancer development, and the mechanism remains unclear [23]. TGF-β mediates cell metastasis through Smad-mediated transcription regulation [24] and non-Smad pathways. The protein level and acetylation ability of p300 are also increased after TGF-β1 stimulation. TGF-β1 enhances the transcription of epithelial-mesenchymal transition (EMT)-related genes by activating transcription factors.

[1]Institute of Cardiovascular Disease of Integrated Traditional Chinese and Western Medicine, Shuguang Hospital, Shanghai University of Traditional Chinese Medicine, Shanghai 201203, China and [2]School of Pharmacy, Shanghai University of Traditional Chinese Medicine, Shanghai 201203, China
Correspondence: Yuan-zhi Lao (laurence_ylao@163.com) or Hong-xi Xu (xuhongxi88@gmail.com)
These authors contributed equally: Jing Wang, Man Wu

Received: 3 January 2019 Accepted: 11 June 2019
Published online: 1 August 2019

Natural compounds play a leading role in the development of anticancer drugs. Recent studies have indicated that some of the natural compounds that target HATs, especially p300, exhibit anticancer activity [25–27]. For instance, allspice extracts and Rosa rugosa methanol extract inhibit both p300 and CBP activity and reduce prostate cancer cell growth [28, 29].

Garcinol, which is extracted from *Garcinia yunnanensis* Hu [30], is regarded as a potent inhibits or HATs, especially p300 [31]. Anti-inflammatory, antioxidation, antitumor, and other activities of Garcinol have been reported [32–34]. Garcinol can reverse the EMT to mesenchymal-epithelial transition via the Wnt signaling pathway in breast cancer [35]. Garcinol can alter the expression and acetylation of the tumor suppressor p53, which results in growth arrest in breast cancer [36]. However, the mechanism by which Garcinol inhibits cell metastasis requires further research, and the process by which p300 mediates downstream signaling and influences cell metastasis has not been reported.

In the present study, we provided evidence that Garcinol inhibits cell migration and invasion by suppressing p300, but not its paralog CBP, and the silencing of p300 can decrease EMT marker protein levels. The TGF-β1-related pathway is also suppressed by Garcinol, and p-Smad2/3, which forms a complex with p300 in the nucleus, is decreased after Garcinol treatment, suggesting that Garcinol is a potent antitumor metastasis drug candidate for preventing and treating esophageal cancer.

MATERIALS AND METHODS

Plant material

Garcinol was obtained from *G. yunnanensis* Hu as previously described [37]. Its structure was determined by ^{1}H-NMR and ^{13}C-NMR spectral analysis, and the purity of Garcinol was more than 98% based on HPLC analysis. This compound was prepared by dissolving in dimethyl sulfoxide (DMSO), and the final concentration of DMSO was adjusted to 0.1% (v/v) in the culture media. DMSO was the control in all cases.

Cell culture

The human esophageal cancer cell lines KYSE150 and KYSE450 were provided by the Fudan University Shanghai Cancer Center. The cells were maintained in a humidified atmosphere containing 5% CO_2 at 37 °C. These cells were cultured in RPMI-1640 (Invitrogen, NY, USA) with 10% fetal bovine serum (FBS, Invitrogen, NY, USA), 100 U/mL penicillin, and 100 mg/mL streptomycin (Invitrogen, NY, USA).

Wound healing assay

A total of 1.5×10^5 cells were seeded into 24-well culture plates. When the cells reached 80%–90% confluence, a scratch was made through the confluent monolayer with a sterile plastic pipette tip. The cells were incubated in fresh complete medium at 37 °C with or without Garcinol and TGF-β1. The migration distance of the cells was monitored and imaged under an Olympus microscope IX83 (Tokyo, Japan).

Transwell and matrigel invasion assays

Cell migration and invasion were determined using a transwell chamber (Corning, NY, USA) with a pore size of 8 μm. For the migration assay, 5×10^4 cells were seeded in FBS-free medium in the upper chamber, and complete medium was added to the lower chamber. For the invasion assay, a total of 2×10^5 cells were plated in serum-free medium in the upper chamber of a Matrigel-coated transwell, and complete medium was added to the lower chamber. After incubation for 24 h at 37 °C, the cells on the upper surface of the chamber were removed using cotton swabs, and then, the migrated cells on the bottom surface were fixed in ethyl alcohol and stained with crystal violet. The membrane was scored under a light microscope in five random fields.

siRNA transfection

The siRNA fusion genes were transfected into KYSE150 cells by Lipofectamine RNAiMAX (Invitrogen, NY, USA), as instructed by the manufacturer. After 24 h of incubation, the cells were subjected to functional evaluations. p300 siRNA (p300-1, 5′-CAGGUAUGAUGAA CAGUCCAGUAAA-3′ and 5′-UUUACUGGACUGUUCAUCAUACCUG-3′; p300-2, 5′-CAGAGCAGUCCUGGAUUAGTT-3′ and 5′-CUAAUCCA GGACUGCUCUGTT-3′; p300-3, 5′-GGAUUCGUCUGUGAUGGCUGUU UAA-3′ and 5′-UUAAACAGCCAUCACAGACGAAUCC-3′), CBP siRNA (CBP-homo-2004, 5′-GGAGCCAUCUAGUGCAUAATT-3′ and 5′-UUA UGCACUAGAUGGCUCCTT-3′; CBP-homo-2209, 5′-GAGGUCGCGU UUACAUAAATT-3′ and 5′-UUUAUGUAAACGCGACCUCTT-3′), and negative control siRNA (5′-UUCUCCGAACGUGUCACGUTT-3′ and 5′-ACGUGACACGUUCGGAGAATT-3′) were purchased from GenePharma.

Western blotting assay

Cells were lysed in RIPA buffer, 1 mM phenylmethanesulfonyl fluoride (PMSF) and protease inhibitor cocktail. The cell extracts were resolved by SDS-PAGE and transferred onto polyvinylidene difluoride membranes. After blocking nonspecific binding with TBS/T (0.1%) containing 5% nonfat milk for 1 h at room temperature, the membranes were probed with the following antibodies: p300 (sc-585, Santa Cruz, CA, USA), CBP (7389, CST, MA, USA), p-Smad2/3 (8828, CST), E-cadherin (3195, CST), vimentin (5741, CST), p-Src (6943, CST), p-AKT (9271, CST), p-MEK (9154, CST), snail (3879 P, CST), α-tubulin (sc-5286, Santa Curz Biotechnology, Santa Curz, CA), and GAPDH (2251, Abcam, Cambridge, UK). Following incubation with horseradish peroxidase-conjugated anti-mouse (074-1806, KPL, MD, USA) or anti-rabbit secondary antibodies (474-1506, KPL), the protein bands were visualized using ECL Blotting Detection Reagents (54-61-00, KPL). The densities of the immunoreactive bands were evaluated using an ATTO Densitograph Software Library CS analyzer (ATTO instruments, Tokyo, Japan).

MTT assay

The cells were treated with various concentrations of Garcinol for 24 h. At the end of the incubation period, 10 μL of 3-(4,5-dimethylthiazol-2-yl)-2,5-diphenyltetrazolium bromide (MTT) solution was added to each well of a 96-well plate for 4 h at 37 °C, and then 150 μL of dimethyl sulfoxide (DMSO) was added to dissolve the purple crystals. The optical densities were measured at 570 nm, and cell viability was normalized as a percentage of the control.

RNA isolation and quantitative RT-PCR

Total RNA isolation was performed using TRIzol reagent (R0016, Beyotime, Jiangsu, China) following the manufacturer's protocol. A total of 2 μg of total RNA was reverse transcribed using the PrimeScript RT Reagent Kit (DRR037A, TaKaRa, Beijing, China). qPCR analysis was performed in a Veriti Thermal Cycler (Applied Biosystems, MA, USA) using SYBR Green master mix (TOYOBO, Osaka, Japan). The human gene primers used in the qPCR reactions were as follows: p300, 5′-AGGGGCAACAAGAAGAAACC-3′ and 5′-AACAATGGGCAGGGA-3′; CBP, 5′-CATCTTCCCAACACCTGA-3′ and 5′-GTCCCCTTCCACTTTCTT-3′; and 18S, 5′-GTAACCCGTTGAAC CCCATT-3′ and 5′-CCATCCAATCGGTAGTAGCG-3′.

Immunofluorescent staining

A total of 5×10^4 cells were grown on glass coverslips overnight and treated with or without 15 μM Garcinol in a culture of 5 ng/mL TGF-β1 for 2, 6, and 12 h. The cells were fixed with 4% paraformaldehyde, washed with PBS for 5 min three times, and then permeabilized using 0.3% Triton X-100 in PBS. After

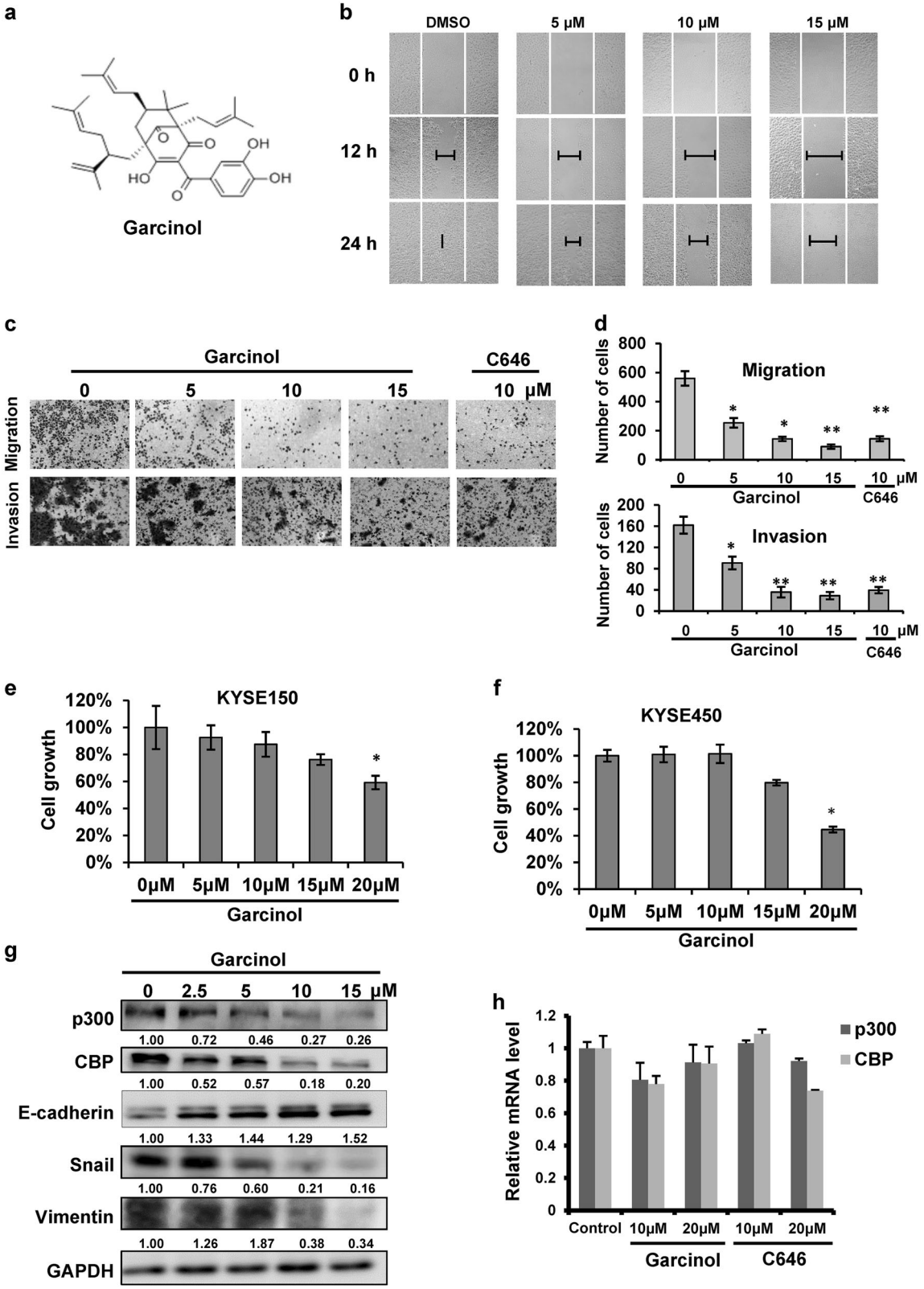

Fig. 1 **a** Chemical structure of Garcinol. **b** KYSE150 cells were scratched and treated with different concentrations of Garcinol for 24 h and then monitored by a microscope. **c** KYSE150 cells were incubated with different concentrations of Garcinol for 24 h, and migrating and invading cells were stained with crystal violet. **d** The number of migrating or invading cells was counted in each group in three independent experiments. **e**, **f** KYSE150 and KYSE450 cells were seeded in 96-well plates, and the cells were incubated in different concentrations of Garcinol for 24 h. **g** KYSE150 cells were incubated in 0, 5, 10 and 15 μM Garcinol for 24 h, and the effects of Garcinol on the protein expression levels of p300, CBP, E-cadherin, vimentin, and snail were detected by Western blotting ($n = 5$). **h** The mRNA levels of p300 and CBP were detected by RT-PCR after Garcinol or C646 treatment. *$P < 0.05$, **$P < 0.01$

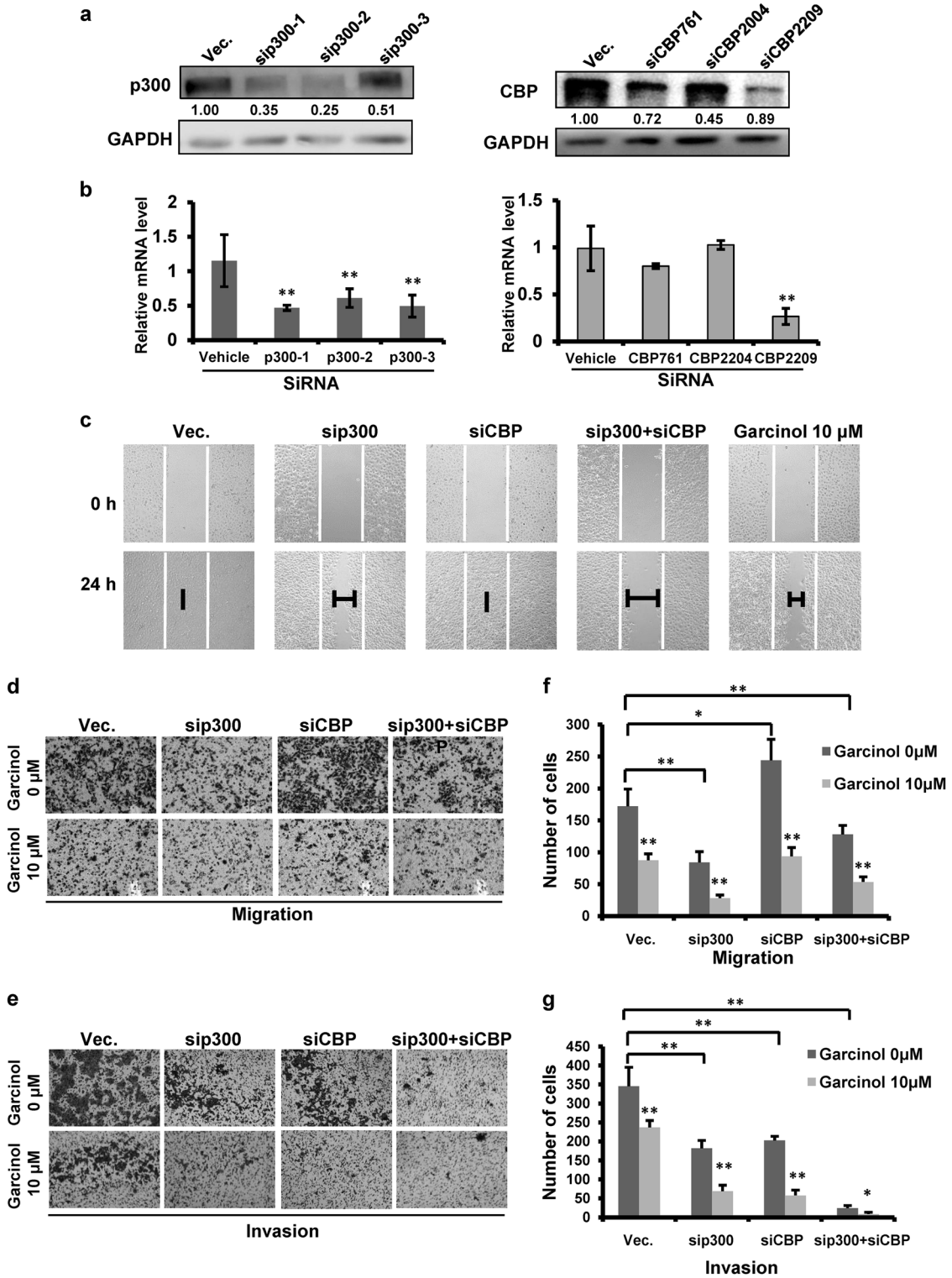

Fig. 2 **a**, **b** KYSE150 cells were transfected with control siRNA, siRNAs (1, 2, and 3) targeting p300 or siRNAs (761, 2204, 2209) targeting CBP for 24 h and analyzed by Western blotting ($n = 5$) and RT-PCR. **c** KYSE150 cells were transfected with siRNA targeting p300 (2), siRNA targeting CBP (2209) or a mixture of siRNAs targeting p300 and CBP for 24 h and then treated with or without 10 μM Garcinol and analyzed with a wound healing assay at 24 h. **d** KYSE150 cells were transfected with siRNA targeting p300 (2), siRNA targeting CBP (2209) or a mixture of siRNAs targeting p300 and CBP. Twenty-four hours after transfection, the cells were seeded into a chamber and treated with or without 10 μM Garcinol for 24 h, and then the migrating cells were stained with crystal violet. **e** KYSE150 cells were transfected with siRNA targeting p300 (2), siRNA targeting CBP (2209) or a mixture of siRNAs targeting p300 and CBP for 24 h. The cells were seeded into Matrigel-coated chambers and treated with or without 10 μM Garcinol for 24 h, and the invading cells were stained with crystal violet. **f**, **g** The number of cells in the Transwell assay (**d**) and the Matrigel invasion assay (**e**) was counted for each group in three independent experiments. The relative protein levels were normalized to GAPDH by using ImageJ software ($n = 5$). The data are presented as the means ± S.D. $^{*}P < 0.05$, $^{**}P < 0.01$

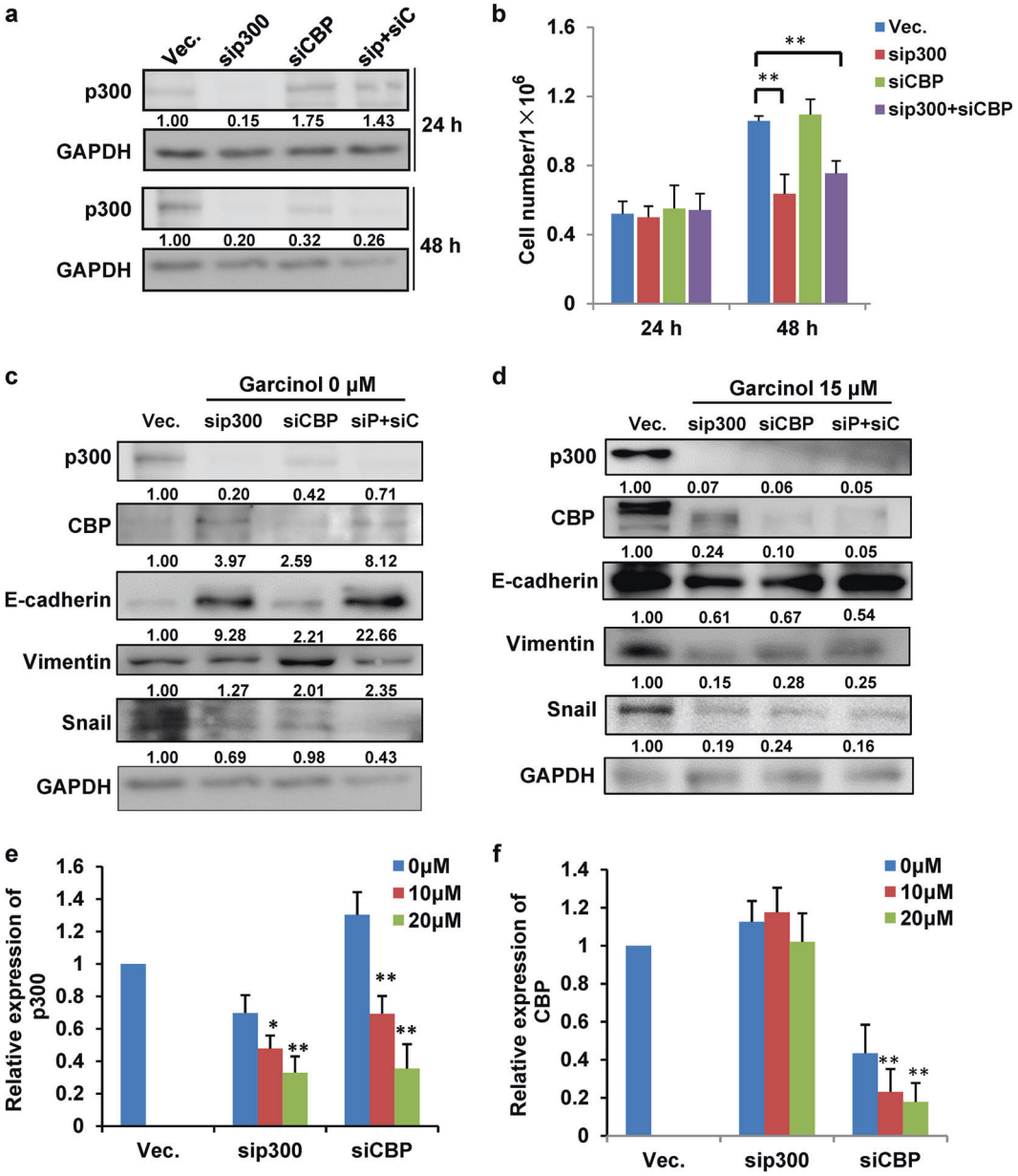

Fig. 3 **a** KYSE150 cells were transfected with siRNA targeting p300, siRNA targeting CBP or a mixture of siRNAs targeting p300 and CBP for the indicated times. The protein levels of p300 at 24 h and 48 h were detected by Western blotting ($n = 5$). **b** Cell viability and the number of cells were analyzed using trypan blue dye staining. The number of cells was counted for each group in three independent experiments ($n = 3$). **c** KYSE150 cells were transfected with siRNA targeting p300 (2), siRNA targeting CBP (2209) or a mixture of siRNAs targeting p300 and CBP for 24 h; p300, CBP, E-cadherin, vimentin, and snail levels were analyzed by Western blotting. **d** KYSE150 cells were transfected with siRNA targeting p300, siRNA targeting CBP or a mixture of siRNAs targeting p300 and CBP and then treated with Garcinol for 24 h; p300, CBP, E-cadherin, vimentin, and snail levels were analyzed by Western blotting ($n = 5$). The relative protein levels were normalized to GAPDH by using ImageJ software. **e**, **f** KYSE150 cells were transfected with siRNA targeting p300 or siRNA targeting CBP and then treated with Garcinol for 24 h. The mRNA levels of p300 and CBP were analyzed. $^{*}P < 0.05$, $^{**}P < 0.01$

permeabilization, the cells were blocked with 5% bovine serum albumin for 1 h and then incubated with a p-Smad2/3 antibody (diluted 1:500) overnight. The coverslips were washed with PBS and then incubated with a Cy3-labeled goat anti-rabbit IgG secondary antibody (diluted 1:500; Beyotime) for 1 h. The coverslips were then washed and mounted using 4′6-diamidino-2-phenylindole, and images were obtained using an Olympus microscope.

Cytosol/membrane fractionation

KYSE150 cells were treated with or without Garcinol for 6, 12, and 24 h. Nuclear and cytoplasmic protein extractions were obtained using the Nuclear and Cytoplasmic Protein Extraction Kit (Beyotime). A protease and phosphatase inhibitor cocktail was added to the protein extract.

Pulmonary metastasis assay in mice

Briefly, 5-week-old male BALC/c nude mice were purchased from the Experimental Animal Center of the Chinese Academy of Science (Shanghai, China) and maintained in a pathogen-free environment. The experimental procedures were approved by the Shanghai University of Traditional Chinese Medicine Committee on the Use of Live Animals for Teaching and Research. The mice were intravenously injected with 1×10^6 KYSE150 cells via the tail

vein. After the injection of the tumor cells, the mice were randomly divided into three groups and received an intraperitoneal injection of saline, Garcinol or 5-fluorouracil (5-FU) once every two days for five weeks.

HE staining and immunohistochemistry

After 35 days of treatment, the mice were sacrificed, and the lungs were immediately removed and fixed in 10% neutral buffered paraformaldehyde at 4 °C for 48 h. Selected samples were embedded in paraffin, sectioned and stained with hematoxylin and eosin. The p300, p-Smad2/3, and Ki-67 primary antibodies were used at 1:100 dilutions. The sections were finally mounted with DPX mountain (317616, Sigma, MO, USA) for histological analysis.

Statistical analysis

Statistical comparisons were performed using Student's *t* test and repeated-measures one-way ANOVA followed by post hoc Dunnett' s test with GraphPad Prism 5 software (GraphPad, CA, USA). Values of $P < 0.05$ were considered significant. All of the results are expressed as the means ± SD, and the experiments were repeated three times independently.

RESULTS

Garcinol inhibits metastasis in ESCC cells

Previous studies showed that Garcinol has the ability to inhibit metastasis in several cancer cell lines, such as HT-29 and PANC-1 cells [38, 39]. Therefore, we examined whether Garcinol affects metastasis in ESCC cells. In the wound healing assay, Garcinol inhibited KYSE150 cell migration at a concentration of 5 μM (Fig. 1b). The inhibitory effects of Garcinol on migration and invasion were investigated using Transwell and Matrigel assays. As shown in Fig. 1c, the number of migrating and invading KYSE150 cells was decreased after treatment with 5, 10, and 15 μM Garcinol, and the compound C646, a commercial p300 inhibitor, was applied as a positive control. The number of migrating and invading cells was counted in Fig. 1d. To eliminate the possibility that the suppression of cell metastasis by Garcinol may be due to the inhibition of cell proliferation, we examined the cytotoxicity of Garcinol in KYSE150 and KYSE450 cells using the MTT assay. Fig. 1e, f shows that 15 μM Garcinol did not suppress cell proliferation, suggesting that Garcinol suppresses cell metastasis. We next determined how Garcinol influences the metastatic signals. As shown in Fig. 1g, Garcinol decreased the protein levels of p300 and CBP in a dose dependent manner. In addition, we observed that Garcinol upregulated the EMT-related protein E-cadherin and downregulated vimentin and snail. The mRNA levels of p300 and CBP were not affected by Garcinol treatment (Fig. 1h). These results suggest that Garcinol inhibits metastasis in ESCC cells.

Garcinol inhibits metastasis in a manner that is dependent on the downregulation of p300

To investigate whether Garcinol affects metastasis by inhibiting p300 and CBP, we evaluated p300/CBP levels upon Garcinol treatment in KYSE150 cells. siRNAs targeting p300 and CBP were transfected into KYSE150 cells, and the protein levels and mRNA levels of p300 and CBP were decreased (Fig. 2a, b). p300-1 siRNA, p300-2 siRNA, and CBP-2209 siRNA were selected for subsequent experiments. The wound healing assay showed that the knockdown of p300 inhibited the migration of KYSE150 cells, but the knockdown of CBP did not (Fig. 2c). The Transwell and Matrigel assays showed similar effects of p300 and CBP siRNA as the wound healing assay. As shown in Fig. 2d, e, the number of migrating and invading cells was further decreased after treatment with 10 μM Garcinol. The statistical analysis of migrating and invading cells is shown in Fig. 2f, g. Thus, the expression of

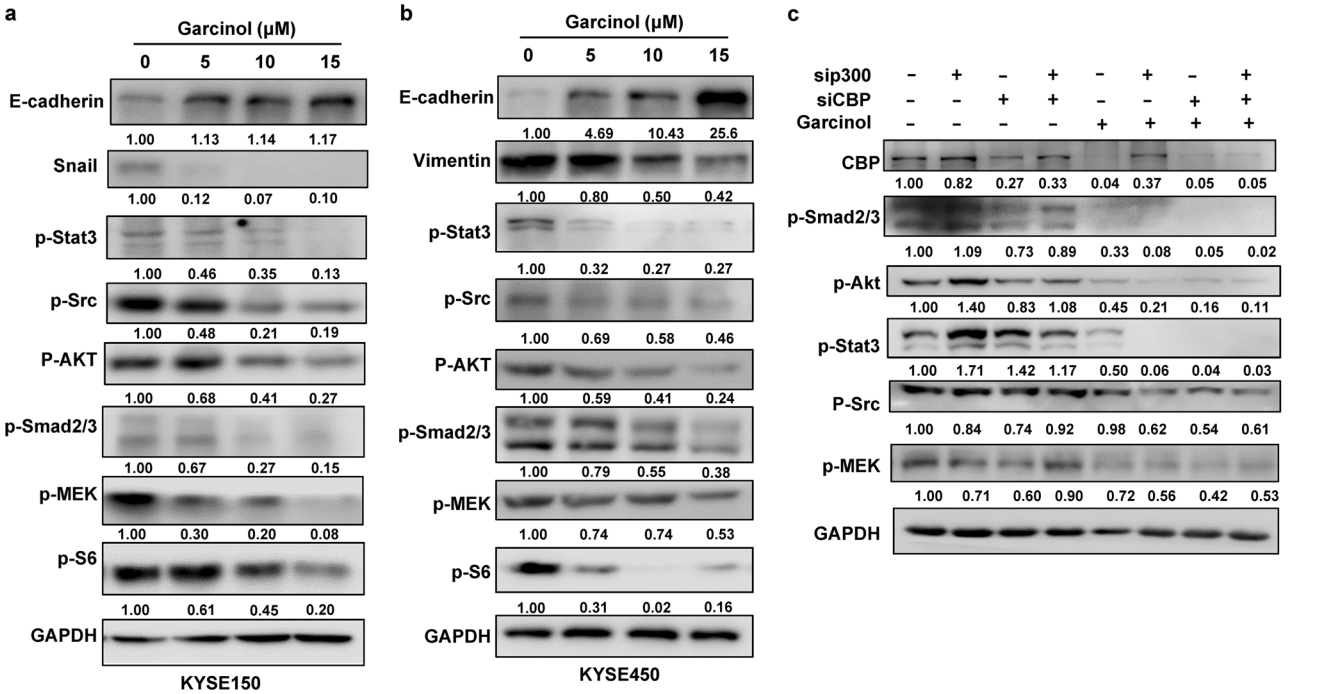

Fig. 4 **a**, **b** KYSE150 and KYSE450 cells were treated with or without Garcinol for 24 h, and E-cadherin, snail, p-Stat3, p-Src, p-AKT, p-Smad2/3, p-MEK, p-S6, and GAPDH proteins were separated and analyzed by Western blotting ($n = 5$). **c** KYSE150 cells were transfected with siRNA targeting p300, siRNA targeting CBP or a mixture of siRNAs targeting p300 and CBP and treated with or without Garcinol for 24 h. p-Stat3, p-Src, p-AKT, p-Smad2/3, p-MEK, and GAPDH levels were analyzed by Western blotting ($n = 5$). The relative protein levels were normalized to GAPDH by using ImageJ software

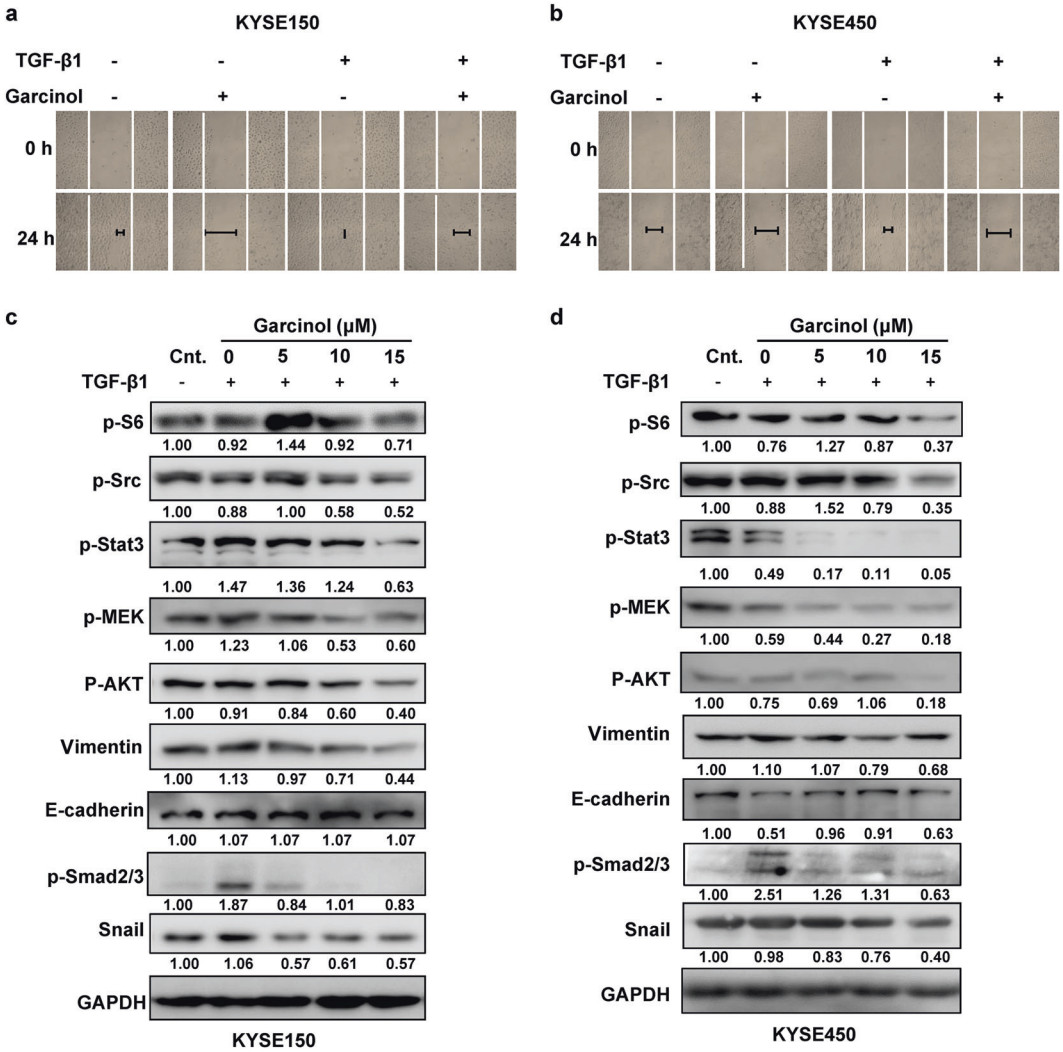

Fig. 5 **a** KYSE150 cells or **b** KYSE450 cells were induced with 5 ng/mL TGF-β1, treated with or without 10 μM Garcinol for 24 h and analyzed by a wound healing assay. **c**, **d** KYSE150 and KYSE450 cells were induced with 5 ng/mL TGF-β1 and treated with different concentrations of Garcinol for 24 h; E-cadherin, snail, p-Stat3, p-Src, p-AKT, p-Smad2/3, p-MEK, p-S6 and GAPDH proteins were separated and analyzed by Western blotting ($n = 5$). The relative protein levels were normalized to GAPDH by using ImageJ software. The data are presented as the means ± SD

p300 is related to the mobility of KYSE150 cells, and the antimetastatic effect of Garcinol may depend on the down-regulation of p300.

We next determined the detailed mechanism of the effect of p300 against metastasis and detected the related changes in proteins after siRNA transfection. The protein levels of p300 and CBP were decreased after transfection with p300 and CBP siRNAs for 24 h and 48 h, and the cell numbers were counted (Fig. 3a, b). The results indicated that the knockdown of p300 suppressed cell growth at 48 h. The expression of the EMT marker was also regulated by p300 and CBP siRNAs. The knockdown of p300 increased the protein level of E-cadherin and decreased the protein level of snail, while the knockdown of CBP did not influence the expression of E-cadherin but decreased the protein level of snail (Fig. 3c). The expression of the EMT marker decreased after p300 knockdown or Garcinol treatment (Fig. 3d). Taken together, our results indicate that p300 is essential for the mediation of KYSE150 cell metastasis and that Garcinol inhibits metastasis by downregulating the expression of p300.

The mRNA levels of p300 and CBP were also determined in p300 and CBP knockdown cells after Garcinol treatment. The expression of p300 mRNA was lower after Garcinol treatment than after vehicle treatment in p300 or CBP knockdown cells (Fig. 3e). However, the expression of CBP mRNA did not change in p300 knockdown cells after Garcinol treatment (Fig. 3f). Garcinol further decreased the expression of p300 mRNA after the knockdown of p300. These data indicate that the metastatic inhibition by Garcinol may be related to the expression of p300 but not CBP.

Garcinol inhibits TGF-β1-induced metastasis in ESCC

p300 and p-Smad2/3 can form a complex in the nucleus and activate downstream metastasis signaling [40]. As shown in Fig. 4a, b, the activation of some protein kinases, including p-Stat3, p-AKT, p-Src, p-Smad2/3, p-MEK, and p-S6, was decreased upon Garcinol treatment in both KYSE150 and KYSE450 cells. The knockdown of p300 increased the protein level of p-Stat3 and decrease the protein level of p-MEK at the same time, but 15 μM Garcinol reversed the expression of p-Stat3 (Fig. 4c).

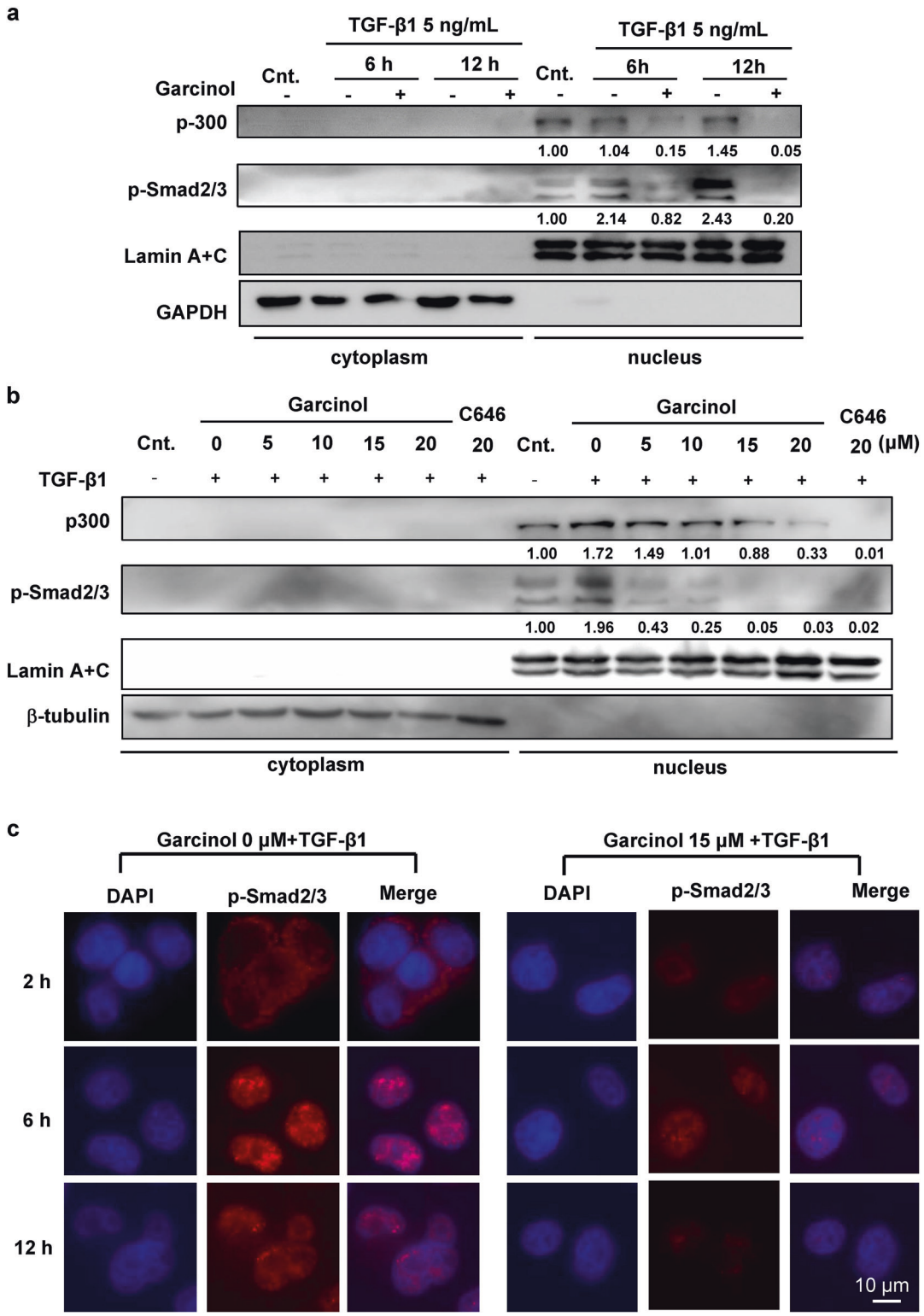

Fig. 6 **a** KYSE150 cells were induced with 5 ng/mL TGF-β1 and treated with or without 15 μM Garcinol for 6 h or 12 h; nuclear and cytosolic proteins were separated using a Nuclear-Cytosol Extraction Kit, and the protein expression levels of p300, p-Smad2/3, lamin A/C and α-tubulin were analyzed by Western blotting ($n = 5$). **b** KYSE150 cells were induced with 5 ng/mL TGF-β1 and incubated with 15 μM Garcinol for 24 h; nuclear and cytosolic proteins were separated using a Nuclear-Cytosol Extraction Kit, and the protein expression levels of p300, p-Smad2/3, lamin A/C and β-tubulin were analyzed by Western blotting ($n = 5$). **c** KYSE150 cells were induced with 5 ng/mL TGF-β1 and treated with or without 15 μM Garcinol for the indicated times, and then images were acquired with a fluorescence microscope with a 60× objective. The scale bars represent 10 μm. The relative protein levels were normalized to GAPDH by using ImageJ software

TGF-β1 can mediate EMT by suppressing the phosphorylation and acetylation of Smad2 and Smad3 in cancer cells [40]. Therefore, we evaluated the expression of proteins downstream of TGF-β1 after Garcinol or p300 siRNA treatment. Garcinol inhibited cell migration with or without TGF-β1 treatment in KYSE150 and KYSE450 cells (Fig. 5a, b). After TGF-β1 simulation for 24 h, Garcinol decreased the protein levels of vimentin, snail, p-Smad2/3, p-Stat3, p-Src, p-AKT, p-MEK, and p-S6 in KYSE150 and KYSE450 cells (Fig. 5c, d). We then determined whether Garcinol can inhibit cell metastasis by inhibiting the nuclear expression of p-Smad2/3. The expression of p-Smad2/3 in the nucleus was decreased in a time- and dose-dependent manner after treatment with Garcinol (Fig. 6a, b). Immunofluorescence staining showed that the expression of p-Smad2/3 was lower after Garcinol treatment for 2, 6, and 12 h (Fig. 6c). Taken together, our data suggest that Garcinol can inhibit TGF-β1-induced metastasis in ESCC.

Garcinol inhibits pulmonary metastasis in mice

To explore the metastatic inhibition effect of Garcinol in vivo, we used a mouse model of pulmonary metastasis induced by tail vein injection. After KYSE150 cells were injected, the mice were randomly divided into three groups and administered vehicle, Garcinol, or 5-FU via intraperitoneal injection ($n = 7$ in each group). Thirty-five days after cell injection, the mice were sacrificed, and pulmonary metastasis was examined by HE and immunohistochemistry staining. As shown in Fig. 7a, lung tumor nodules were observed in the control group, whereas both

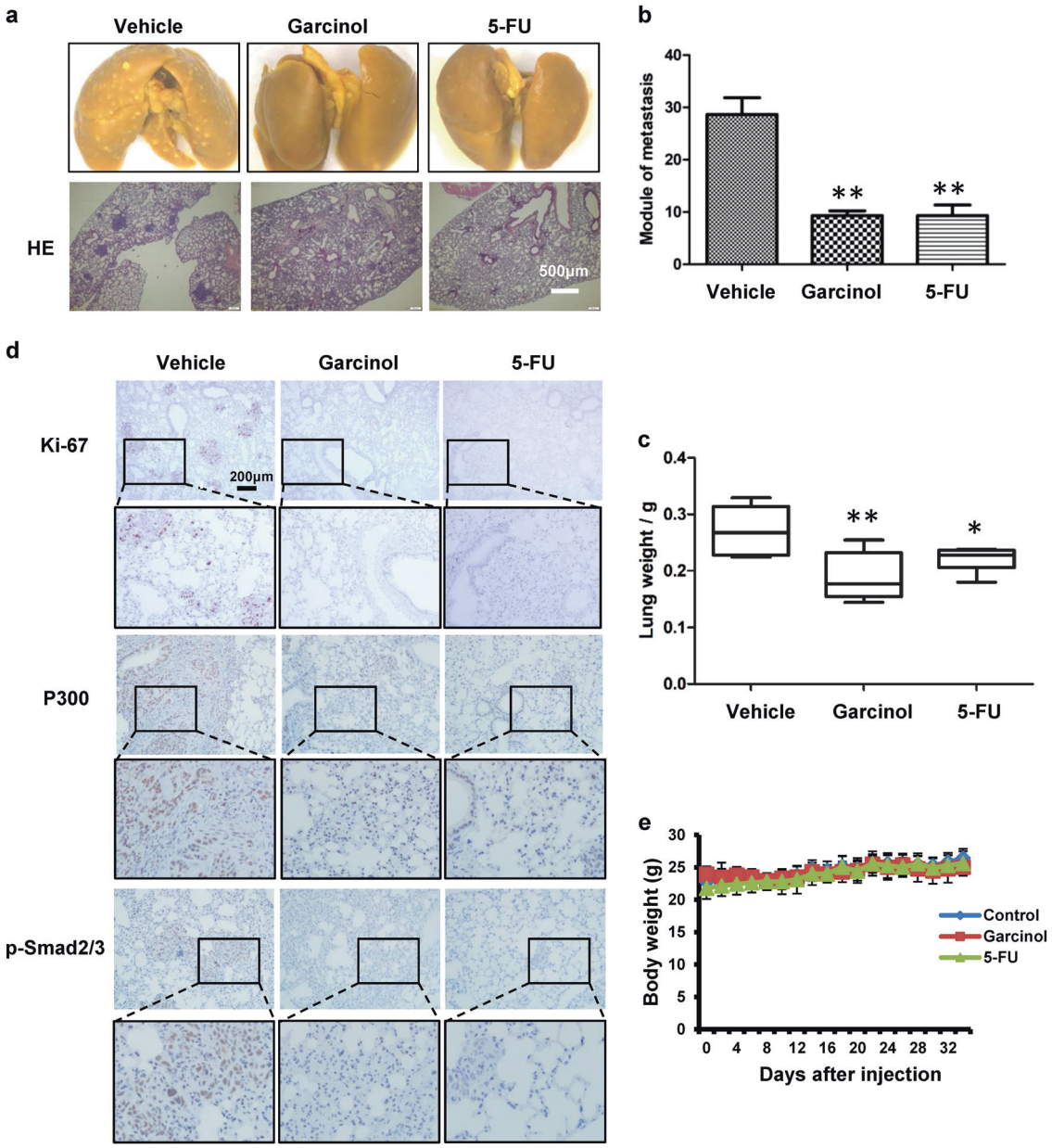

Fig. 7 Garcinol inhibits pulmonary tumor metastasis in mice. **a** Six-week-old male nude mice were injected into the tail vein with 1×10^6 KYSE150 cells. After injection, the mice were divided into three groups: the vehicle group, the Garcinol-treated (20 mg/kg per 2 days) group and the 5-FU-treated (20 mg/kg per 2 days) group ($n = 7$ in each group). Representative examples and HE staining of lungs from each group after 5 weeks. **b** Quantitative analysis of metastatic nodes in lung. $^*P < 0.05$, $^{**}P < 0.01$. **c** Lung weight, as analyzed after treatment. $^*P < 0.05$, $^{**}P < 0.01$. **d** Immunohistochemical staining for Ki-67, p300 and p-Smad2/3 in lung tissues. **e** Body weights were analyzed every two days throughout the experiment

Garcinol and 5-FU reduced the number of tumor nodules. The quantitative analysis is shown in Fig. 7b; the number of nodules in the Garcinol- and 5-FU-treated groups was significantly decreased compared with that in the vehicle group. The weight of the lungs in the Garcinol and 5-FU treated groups was decreased compared to that in the vehicle group (Fig. 7c). Ki-67 is a marker of cell proliferation, and the inhibition of Ki-67 expression leads to the suppression of proliferation. After Garcinol or 5-FU injection, the expression of Ki-67 was lower than that after vehicle injection, as was 5-FU (Fig. 7d). Consistent with the in vitro experiments, Garcinol did not have significant effects on the weight of the mice (Fig. 7e) or other tissues. After Garcinol or 5-FU injection, the levels of p300 and p-Smad2/3 were also decreased in the lung tissues (Fig. 7d). In summary, our study indicates that Garcinol is an interesting natural compound that affects non-Smad and Smad pathways in esophageal cancer cells.

DISCUSSION

p300 and CBP function as transcriptional cofactors and HATs. The high expression of p300 is associated with poor survival in esophageal cancer patients, and p300 has been an important drug target in cancer research [41]. In this study, we found that Garcinol may be an active metastatic inhibitor in esophageal cancers. Garcinol may be an effective inhibitor of tumor metastasis, and its effect was investigated by using wound healing, Transwell migration and invasion assays. Our data also suggested that Garcinol inhibits p300 and CBP without downregulating their mRNA levels (Fig. 1h). Our further studies indicated that Garcinol inhibits TGF-β1 signaling pathways, including Smad and non-Smad pathways. Phosphorylated Smad2 and Smad3 are associated with Smad4, translocate to the nucleus and act as transcription factors [42]. Garcinol treatment leads to a decrease in p-Smad2/3 and p300 in the nucleus, which causes the downregulation of EMT markers.

p300 and CBP have multiple functional domains that accommodate diverse protein–protein interactions to enable a large number of disparate transcription factors [43]. Although p300/CBP have been implicated in cancer development, the specific mechanisms have been less precisely defined [44]. Research has shown that p300 promotes proliferation, migration, and invasion in NSCLC [45]. The overexpression of p300 is a poor prognostic factor in breast cancer, prostate cancer, hepatocellular carcinoma, and esophageal squamous cell carcinoma [46–48]. In our previous studies, we found that Garcinol has a potential effect on p300 and CBP, leads to p-Stat3, p-Src and p-AKT downregulation, and inhibits EMT functions and characteristics. Then, we investigated the role of p300/CBP in inhibiting ESCC metastasis, and the results indicated that p300, but not CBP, has an antimetastatic effect. We also made an attempt to overexpress p300 to explore its effect. However, due to the high molecular weight of p300, it was difficult to obtain sufficient effective and convincing experimental results; we will try to verify the results in the future. In our animal study, compared to the positive control 5-FU, Garcinol inhibited pulmonary metastasis (Fig. 7).

TGF-β1 stimulation results in the phosphorylation of the (Serine-Serine-X-Serine) SSXS motif of Smad2 and Smad3, which leads to nuclear translocation [49]. Both Smad2 and Smad3 directly interact with p300/CBP in the nucleus [50]. In this study, we determined that the phosphorylation of Smad2 and Smad3 can be suppressed by Garcinol, which can also decrease the p300 protein level in the nucleus. This activity of p300/CBP is considered a novel target for the prevention of EMT and fibrosis [51]. TGF-β1 can upregulate the acetyltransferase activity of p300 in some sensitive ESCC cells, in which Garcinol inhibits the stimulation of p300 activity by TGF-β1 [49]. The results suggested that the regulation of TGF-β1 signaling by Garcinol is also important for the chemoprevention of invasion and metastasis in cancer. Thus, our findings highlight that p300/CBP and Smad2/Smad3 in the TGF-β1 signaling pathway are essential components for the regulation of the TGF-β1-induced transcriptional activation of EMT markers in human ESCC cells (Fig. 6).

In conclusion, we demonstrated that Garcinol can inhibit p300 and p-Smad2/3 in the nucleus to block the transcription of metastasis-related genes. We also found that the knockdown of p300 can downregulate p-MEK and p-S6, which are related to EMT. Garcinol can also suppress Smad and non-Smad pathways, which are activated by TGF-β1. Thus, Garcinol decreases EMT marker gene expression by inhibiting the TGF-β1 pathway and p300. As a result, our findings reveal a new mechanism by which Garcinol inhibits cell metastasis through the inhibition of p300 and p-Smad2/3 activity in human ESCC cells.

ACKNOWLEDGEMENTS

This work was supported by National Natural Science Foundation of China (Nos. 81773951 and 81303188) and the three-year development plan project for Traditional Chinese Medicine (ZY(2018-2020)-CCCX-2001-02) to HXX.

AUTHOR CONTRIBUTIONS

JW and MW contributed equally. Study concept and design: YZL, HXX and JW; chemical synthesis and micelle characterization: DZ, HZ and HST; biological study: JW, MW and LZ; analysis of data: JW, MW, HZ, and YL; drafting of the manuscript: JW and MW.

ADDITIONAL INFORMATION

Competing interests: The authors declare no competing interests.

REFERENCES

1. Murphy G, McCormack V, Abedi-Ardekani B, Arnold M, Camargo MC, Dar NA, et al. International cancer seminars: a focus on esophageal squamous cell carcinoma. Ann Oncol. 2017;28:2086–93.
2. Malhotra GK, Yanala U, Ravipati A, Follet M, Vijayakumar M, Are C. Global trends in esophageal cancer. J Surg Oncol. 2017;115:564–79.
3. Zeng H, Zheng R, Guo Y, Zhang S, Zou X, Wang N, et al. Cancer survival in China, 2003–2005: a population-based study. Int J Cancer. 2015;136:1921–30.
4. Siegel RL, Miller KD, Jemal A. Cancer statistics. 2018. CA. 2018;68:7–30.
5. De Angelis R, Sant M, Coleman MP, Francisci S, Baili P, Pierannunzio D, et al. Cancer survival in Europe 1999-2007 by country and age: results of EUROCARE–5-a population-based study. Lancet Oncol. 2014;15:23–34.
6. Enzinger PC, Mayer RJ. Esophageal cancer. N Engl J Med. 2003;349:2241–52.
7. Steeg PS. Tumor metastasis: mechanistic insights and clinical challenges. Nat Med. 2006;12:895–904.
8. Hirano H, Boku N. The current status of multimodality treatment for unresectable locally advanced esophageal squamous cell carcinoma. Asia Pac J Clin Oncol. 2018;14:291–99.
9. van Hagen P, Hulshof MC, van Lanschot JJ, Steyerberg EW, van Berge Henegouwen MI, Wijnhoven BP, et al. Preoperative chemoradiotherapy for esophageal or junctional cancer. N Engl J Med. 2012;366:2074–84.
10. Kato H, Nakajima M. Treatments for esophageal cancer: a review. Gen Thorac Cardiovasc Surg. 2013;61:330–5.
11. Ito T. Role of histone modification in chromatin dynamics. J Biochem. 2007; 141:609–14.
12. Peserico A, Simone C. Physical and functional HAT/HDAC interplay regulates protein acetylation balance. J Biomed Biotechnol. 2011;2011:371832.
13. Grunstein M. Histone acetylation in chromatin structure and transcription. Nature. 1997;389:349–52.
14. Asaduzzaman M, Constantinou S, Min H, Gallon J, Lin ML, Singh P, et al. Tumour suppressor EP300, a modulator of paclitaxel resistance and stemness, is downregulated in metaplastic breast cancer. Breast Cancer Res Treat. 2017;163: 461–74.
15. Chang R, Zhang Y, Zhang P, Zhou Q. Snail acetylation by histone acetyltransferase p300 in lung cancer. Thorac Cancer. 2017;8:131–37.
16. Giotopoulos G, Chan WI, Horton SJ, Ruau D, Gallipoli P, Fowler A, et al. The epigenetic regulators CBP and p300 facilitate leukemogenesis and represent therapeutic targets in acute myeloid leukemia. Oncogene. 2016;35:279–89.

17. Bordonaro M, Lazarova DL. Determination of the role of CBP- and p300-mediated Wnt signaling on colonic cells. JMIR Res Protoc. 2016;5:e66.
18. Gao Y, Geng J, Hong X, Qi J, Teng Y, Yang Y, et al. Expression of p300 and CBP is associated with poor prognosis in small cell lung cancer. Int J Clin Exp Pathol. 2014;7:760–7.
19. Li Y, Yang HX, Luo RZ, Zhang Y, Li M, Wang X, et al. High expression of p300 has an unfavorable impact on survival in resectable esophageal squamous cell carcinoma. Ann Thorac Surg. 2011;91:1531–8.
20. Liang Y, Wu Y, Chen X, Zhang S, Wang K, Guan X, et al. A novel long noncoding RNA linc00460 upregulated by CBP/P300 promotes carcinogenesis in Esophageal Squamous Cell Carcinoma. Biosci Rep. 2017;37:BSR20171019.
21. Gray SG, Teh BT. Histone acetylation/deacetylation and cancer: an "open" and "shut" case? Curr Mol Med. 2001;1:401–29.
22. Liu N, Li S, Wu N, Cho KS. Acetylation and deacetylation in cancer stem-like cells. Oncotarget. 2017;8:89315–25.
23. Ikushima H, Miyazono K. TGFbeta signalling: a complex web in cancer progression. Nat Rev Cancer. 2010;10:415–24.
24. Feng XH, Derynck R. Specificity and versatility in tgf-beta signaling through Smads. Annu Rev Cell Dev Biol. 2005;21:659–93.
25. Newman DJ, Cragg GM. Natural products as sources of new drugs over the 30 years from 1981 to 2010. J Nat Prod. 2012;75:311–35.
26. Shah U, Shah R, Acharya S, Acharya N. Novel anticancer agents from plant sources. Chin J Nat Med. 2014;11:16–23.
27. Liao ZW, Zhao L, Cai MY, Xi M, He LR, Yu F, et al. P300 promotes migration, invasion and epithelial-mesenchymal transition in a nasopharyngeal carcinoma cell line. Oncol Lett. 2017;13:763–69.
28. Lee YH, Hong SW, Jun W, Cho HY, Kim HC, Jung MG, et al. Anti-histone acetyltransferase activity from allspice extracts inhibits androgen receptor-dependent prostate cancer cell growth. Biosci Biotechnol Biochem. 2007;71:2712–9.
29. Lee YH, Jung MG, Kang HB, Choi KC, Haam S, Jun W, et al. Effect of anti-histone acetyltransferase activity from Rosa rugosa Thunb. (Rosaceae) extracts on androgen receptor-mediated transcriptional regulation. J Ethnopharmacol. 2008;118:412–7.
30. Zheng D, Zhang H, Zheng CW, Lao YZ, Xu DQ, Xiao LB, et al. Garciyunnanimines A–C, novel cytotoxic polycyclic polyprenylated acylphloroglucinol imines from *Garcinia yunnanensis*. Org Chem Front. 2017;4:2102–8.
31. Balasubramanyam K, Altaf M, Varier RA, Swaminathan V, Ravindran A, Sadhale PP, et al. Polyisoprenylated benzophenone, garcinol, a natural histone acetyltransferase inhibitor, represses chromatin transcription and alters global gene expression. J Biol Chem. 2004;279:33716–26.
32. Calabrese V, Boyd-Kimball D, Scapagnini G, Butterfield DA. Nitric oxide and cellular stress response in brain aging and neurodegenerative disorders: the role of vitagenes. In Vivo. 2004;18:245–67.
33. Mathijssen RHJ, van Alphen RJ, Verweij J, Loos WJ, Nooter K, Stoter G, et al. Clinical pharmacokinetics and metabolism of irinotecan (CPT-11). Clin Cancer Res. 2001;7:2182–94.
34. Lakshmi C, Kumar KA, Dennis TJ, Kumar TSSPNSS. Antibacterial activity of polyphenols of *Garcinia indica*. Indian J Pharm Sci. 2011;73:470–2.
35. Ahmad A, Sarkar SH, Bitar B, Ali S, Aboukameel A, Sethi S, et al. Garcinol regulates EMT and Wnt signaling pathways in vitro and in vivo, leading to anticancer activity against breast cancer cells. Mol Cancer Ther. 2012;11:2193–201.
36. Collins HM, Abdelghany MK, Messmer M, Yue B, Deeves SE, Kindle KB, et al. Differential effects of garcinol and curcumin on histone and p53 modifications in tumour cells. BMC Cancer. 2013;13:37.
37. Xu G, Feng C, Zhou Y, Han QB, Qiao CF, Huang SX, et al. Bioassay and ultra-performance liquid chromatography/mass spectrometry guided isolation of apoptosis-inducing benzophenones and xanthone from the pericarp of *Garcinia yunnanensis* Hu. J Agric Food Chem. 2008;56:11144–50.
38. Parasramka MA, Ali S, Banerjee S, Deryavoush T, Sarkar FH, Gupta S. Garcinol sensitizes human pancreatic adenocarcinoma cells to gemcitabine in association with microRNA signatures. Mol Nutr Food Res. 2013;57:235–48.
39. Chen X, Zhang X, Lu Y, Shim JY, Sang S, Sun Z, et al. Chemoprevention of 7,12-dimethylbenz[a]anthracene (DMBA)-induced hamster cheek pouch carcinogenesis by a 5-lipoxygenase inhibitor, garcinol. Nutr Cancer. 2012;64:1211–18.
40. Tu AW, Luo K. Acetylation of Smad2 by the co-activator p300 regulates activin and transforming growth factor beta response. J Biol Chem. 2007;282:21187–96.
41. Lasko LM, Jakob CG, Edalji RP, Qiu W, Montgomery D, Digiammarino EL, et al. Discovery of a selective catalytic p300/CBP inhibitor that targets lineage-specific tumours. Nature. 2017;550:128–32.
42. Hayashi H, Abdollah S, Qiu Y, Cai J, Xu YY, Grinnell BW, et al. The MAD-related protein Smad7 associates with the TGFbeta receptor and functions as an antagonist of TGFbeta signaling. Cell. 1997;89:1165–73.
43. Chakravarti D, Ogryzko V, Kao HY, Nash A, Chen H, Nakatani Y, et al. A viral mechanism for inhibition of p300 and PCAF acetyltransferase activity. Cell. 1999;96:393–403.
44. Attar N, Kurdistani SK. Exploitation of EP300 and CREBBP lysine acetyltransferases by cancer. Cold Spring Harb Perspect Med. 2017;7:a026534.
45. Hou X, Gong R, Zhan J, Zhou T, Ma Y, Zhao Y, et al. p300 promotes proliferation, migration, and invasion via inducing epithelial-mesenchymal transition in non-small cell lung cancer cells. BMC Cancer. 2018;18:641.
46. Zhang C, Li K, Wei L, Li Z, Yu P, Teng L, et al. p300 expression repression by hypermethylation associated with tumour invasion and metastasis in oesophageal squamous cell carcinoma. J Clin Pathol. 2007;60:1249–53.
47. Li M, Luo RZ, Chen JW, Cao Y, Lu JB, He JH, et al. High expression of transcriptional coactivator p300 correlates with aggressive features and poor prognosis of hepatocellular carcinoma. J Transl Med. 2011;9:5.
48. Debes JD, Sebo TJ, Lohse CM, Murphy LM, Haugen DA, Tindall DJ. p300 in prostate cancer proliferation and progression. Cancer Res. 2003;63:7638–40.
49. Asano Y, Czuwara J, Trojanowska M. Transforming growth factor-beta regulates DNA binding activity of transcription factor Fli1 by p300/CREB-binding protein-associated factor-dependent acetylation. J Biol Chem. 2007;282:34672–83.
50. Kawabata M, Imamura T, Inoue H, Hanai J, Nishihara A, Hanyu A, et al. Intracellular signaling of the TGF-beta superfamily by Smad proteins. Ann N Y Acad Sci. 1999;886:73–82.
51. Ghosh AK, Vaughan DE. Fibrosis: is it a coactivator disease? Front Biosci (Elite Ed). 2012;4:1556–70.